J|A|C|S
ARTICLES
Published on Web 02/04/2003

Nanoscopic Assemblies between Supramolecular Redox Active Metallodendrons and Gold Nanoparticles: Synthesis, Characterization, and Selective Recognition of $H_2PO_4^-$, HSO_4^-, and Adenosine-5′-Triphosphate (ATP^{2-}) Anions

Marie-Christine Daniel,[†] Jaime Ruiz,[†] Sylvain Nlate,[†] Jean-Claude Blais,[‡] and Didier Astruc*,[†]

Contribution from the Groupe Nanoscience et Catalyse, LCOO, UMR CNRS No. 5802, Université Bordeaux I, 33405 Talence Cedex, France and LCSOB, UMR CNRS No. 7613, Université Paris VI, 75252 Paris, France

Received November 1, 2002; E-mail: d.astruc@lcoo.u-bordeaux.fr

Abstract: Tri- and nonaferrocenyl thiol dendrons have been synthesized and used to assemble dendronized gold nanoparticles either by the ligand-substitution method from dodecanethiolate−gold nanoparticles (AB_3 units) or Brust-type direct synthesis from a 1:1 mixture of dodecanethiol and dendronized thiol (AB_9 units). The dendronized colloids are a new type of dendrimers with a gold colloidal core. Two colloids containing a nonasilylferrocenyl dendron have been made; they bear respectively 180 and 360 ferrocenyl units at the periphery. These colloids selectively recognize the anions $H_2PO_4^-$ and adenosine-5′-triphosphate (ATP^{2-}) with a positive dendritic effect and can be used to titrate these anions because of the shift of the CV wave even in the presence of other anions such as Cl^- and HSO_4^-. Recognition is monitored by the appearance of a new wave at a less positive potential in cyclic voltammetry (CV). The anion HSO_4^- is also recognized and titrated by the dendronized colloid containing the tris-amidoferrocenyl units, because of the progressive shift of the CV wave until the equivalence point. These dendronized colloids can form robust modified electrodes by dipping the naked Pt electrode into a CH_2Cl_2 solution containing the colloids. The robustness is all the better as the dendron is larger. These modified electrodes can recognize $H_2PO_4^-$, ATP^{2-} and HSO_4^-, be washed with minimal loss of adsorbed colloid, and be reused.

Introduction

Nanoscopic supramolecular assemblies[1] between dendrimers[2] and colloids[3] should be fruitful to provide a new generation of materials that are likely to give applications as sensors,[1,4,5] catalysts,[1,3,6] and components for molecular electronics.[1,7] So far, only very few examples of assemblies between dendrimers or dendrons[8] and colloids are known.[1,9] We have been interested in such assemblies disclosing supramolecular properties in order to provide means to approach new sensors. The recognition of anions has indeed been the subject of special scrutiny, given their role in biology.[10] In particular, Beer has shown various examples of redox anion recognition by amidoferrocenes bound to endoreceptors.[11] We have addressed the use of redox-active

† University Bordeaux I. This article is part of the Ph.D. thesis of M.-C.D.

‡ University Paris VI (MALDI TOF mass spectroscopy).

(1) (a) Balogh, L.; Tomalia, D. A. *J. Am. Chem. Soc*. **1998**, *120*, 7355. (b) Zhao, M.; Crooks, R. M. *Angew. Chem., Int. Ed*. **1999**, *38*, 364. (c) Niu, Y.; Yeung, L. K.; Crooks, R. M. *J. Am. Chem. Soc* **2001**, *123*, 6840. (d) Crooks, R. M.; Zhao, M.; Sun, L.; Chechik, V.; Yeung, L. K. *Acc. Chem. Res*. **2001**, *34*, 181.

(2) (a) Tomalia, D. A.; Naylor, A. N.; Goddard, W. A., III *Angew. Chem., Int. Ed. Engl.* **1990**, *29*, 138. (b) Ardoin, N.; Astruc, D. *Bull. Soc. Chim. Fr*. **1995**, *132*, 875. (c) Matthews, O. A.; Shipway, A. N.; Stoddart, J. F. *Prog. Polym. Chem*. **1998**, *23*, 1. (d) Smith, D. K.; Diederich, F. *Angew. Chem. Eur. J.* **1998**, *4*, 1353. (e) Balzani, V.; Campagna, S.; Denti, G.; Juris, A.; Serroni, S.; Venturi, M. *Acc. Chem. Res*. **1998**, *31*, 26. (f) Gossage, R. A.; van de Kuil, L. A.; van Koten, G. *Acc. Chem. Res*. **1998**, *31*, 423. (g) Bosman, A. W.; Jansen, E. W.; Meijer, E. W. *Chem. Rev.* **1999**, *99*, 1665. (h) Fisher, M.; Vögtle, F. *Angew. Chem., Int. Ed.* **1999**, *38*, 884. (i) Hecht, S.; Fréchet, J. M. J. *Angew. Chem., Int. Ed.* **2001**, *40*, 74. (j) Balzani, V.; Ceroni, P.; Juris, A.; Venturi, M.; Campagna, S.; Puntoriero, F.; Serroni, S. *Coord. Chem. Rev.* **2001**, 219−221, 545. (k) Newkome, G. R.; Moorefield, C. N.; Vögtle, F. *Dendrimers and Dendrons: Concepts, Syntheses, Applications;* Wiley-VCH: Weinheim, Germany, 2001.

(3) (a) Schmid, G. *Chem. Rev.* **1992**, *92*, 1709. (b) Bradley, J. S. In *Clusters and Colloïds*; Schmid, G., Ed.; VCH: Weinheim, Germany, 1995; Chapter 6. (c) Schmid, G.; Chi, L. F. *Adv. Mater*. **1998**, *18*, 515.

(4) (a) Schierbaum, K. D.; Weiss, T.; Thorden van Zelzen, E. U.; Engberson, J. F. G.; Reinhoudt, D. N.; Göpel, W. *Science* **1994**, *265*, 1413. (b) Chechik, V.; Crooks, R. M. *Langmuir* **1999**, *15*, 6364. (c) Garcia, M. E.; Baker, L. A.; Crooks, R. M. *Anal. Chem.* **1999**, *71*, 256.

(5) Daniel, M.-C.; Ruiz, J.; Nlate, S.; Palumbo, J.; Blais, J.-C.; Astruc, D. *Chem. Commun*. **2001**, 2000.

(6) Astruc, D.; Chardac, F. *Chem. Rev.* **2001**, *101*, 2991.

(7) (a) Lehn, J.-M. *Supramolecular Chemistry: Concepts and Perspectives;* VCH: Weinheim, Germany, 1995. (b) Kumar, A.; Arbott, N. L.; Kim, E.; Biebuyck, A.; Whitesides, G. M. *Acc. Chem. Res.* **1995**, *28*, 219. (c) *Nanosystems, Molecular Machinery, Manufactoring and Computation;* Drexler, K. E., Ed.; Wiley: New York, 1992. (d) Willner, I.; Willner, B. *Adv. Mater*. **1997**, *9*, 351.

(8) For a comprehensive review on dendrons, see: Grayson, S. M.; Fréchet, J. M. J. *Chem. Rev.* **2001**, *101*, 3819.

(9) For previous dendron-colloid assemblies, see: ref 5 and (a) Kim, M. K.; Jeon, Y.-M.; Jeon, W. S.; Kim, H.-J.; Hong, S. G.; Park, C. G.; Kim, K. *Chem. Commun*. **2001**, 667. (b) Wang, R.; Yang, J.; Zheng, Z.; Carducci, M. D. *Angew. Chem., Int. Ed.* **2001**, *40*, 549.

(10) Seel, C.; de Mendoza, J. In *Comprehensive Supramolecular Chemistry*; Atwood, J., Davies, J. E. D., McNichol, D. D., Vögtle, F. Eds.; Elsevier: New York, 1996; Vol. 2, Chapter 17, pp 519−552.

(11) (a) Beer, P. D. *Adv. Inorg. Chem*. **1992**, *39*, 79. (b) Beer, P. D. *J. Chem. Soc., Chem. Commun.* **1996**, 689. (c) Beer, P. D. *Acc. Chem. Res.* **1998**, *31*, 71. (d) Beer, P. D.; Gale, P. A.; Chen, Z. *Adv. Phys. Org. Chem*. **1998**, *31*, 1. (e) Beer, P. D.; Gale, P. A. *Angew. Chem., Int. Ed.* **2001**, *40*, 486.

10.1021/ja021325d CCC: $25.00

metallodendrimers[12a,b] and colloids[5,12c,d] as *exo*-receptors for the recognition of anions. Dendrimers show positive dendritic effects, that is, the recognition improves as the generation number increases, because the redox centers become close to one another at the periphery for high generations.[12a,b] On the other hand, colloids are also relatively good sensors that present the advantage over dendrimers that they are rapidly prepared, although the magnitude of the recognition phenomena only reaches that of low-generation dendrimers.[5,12c,d] Thus, the novel assemblies between supramolecular dendrons containing redox-active groups and colloids should disclose new features involving hopefully good recognition properties. We already know that AB_3 units bearing thiol functions and three amido- or silylferrocenyl groups can be introduced to a certain extent onto gold colloids by the classic ligand-substitution procedure that leaves the core intact.[5] These colloids do recognize $H_2PO_4^-$ as well as or slightly better than gold colloids containing thiol ligands bearing a single amidoferrocenyl unit.[12c] We now report the extension of these studies to direct synthetic methods of assemblies between gold colloids and two real dendrons (AB_9 units) containing nine ferrocenyl groups. This allows us to compare assemblies containing colloid-AB_3 units and colloid-AB_9 dendrons for the recognition of $H_2PO_4^-$. We have also now applied these principles to the recognition of the biologically important adenosine-5′-triphosphate anion (ATP^{2-}). Finally, we also present here successful attempts specific to these assemblies to prepare stable derivatized electrodes that also recognize these anions. So far, only very few other examples of molecular recognition by nanoparticles have been reported,[13−17] although ferrocenyl-alkylthiol ligands bonded to surfaces in self-assembled monolayers and particles have been known for some time.[18] Fitzmaurice and Stoddart et al. have shown the recognition of dibenzylammonium cation using crown ethers located at the periphery of nanoparticles.[13] Rotello et al. have investigated supramolecular recognition between flavin and the diacetyl derivative of diamidopyridine.[15] Thiol-modified oligonucleotides have been fixed onto gold nanoclusters. In particular, Mirkin and Letsinger have used such modified nanoparticles for several studies involving DNA analysis,[16] and Mann et al have built three-dimensional networks by antigen−antibody associations.[17] Recently, Nishihara has reported a series of studies on gold nanoparticles bonded to thiolate ligands bearing mixed-valent biferrocenyl (AB_2) units.[19]

Results and Discussions

We have used two synthetic strategies to introduce the AB_3 and AB_9 units onto the colloids. The first one is the exchange of a limited proportion of alkylthiol ligands in Brust-type alkylthiol−gold colloids.[18c,20] This method was already involved to introduce amidoferrocenylalkylthiols in our preliminary work.[12c] It has the advantage of keeping the core size unchanged during the ligand-substitution reaction, but the proportion of substituted ligands can be small with dendrons that are much bulkier than linear thiols. The other one is new, exploratory, and consists of a direct synthesis,[20] derived from Brust's method, for which both dodecanelthiol and dendronized alkylthiols are allowed to competitively react during the direct colloid synthesis. These two synthetic approaches of the supramolecular colloids have been applied to the AB_3 and AB_9 units and compared.

Synthesis of the Dendronized Thiol Ligands. (a) AB_3 Units. The synthesis starts with the phenoltriallyl derivative **1**. This compound is an AB_3 unit that is now easily available in good yield from $[FeCp(\eta^6\text{-}p.MeC_6H_4OEt)][PF_6]$, itself synthesized in large scale from $[FeCp(\eta^6\text{-}p.MeC_6H_4Cl)][PF_6]$, ethanol, and potassium carbonate.[21] A convenient entry into functionalized dendrons derived from **1** is the direct hydrosilylation with various silanes[22,23] of the three allyl groups of **1** without any protection of the phenol function, as exemplified in Scheme 1 for the synthesis of **2** and **3** (top). The following organic reactions also proceed in good yields to provide the phenol compound **6** derived with three amidoferrocenyl groups. The introduction of the thiol group into these dendrons **2** and **6** was achieved by selective reaction with *p*.di(bromomethyl)benzene (in excess) giving **7** and **9** followed by reaction with NaSH which finally yielded **8** and **10**. These new functional thiols are very air sensitive and are quickly oxidized to the corresponding disulfide in air, possibly because the ferrocenyl groups act as redox catalysts for this aerobic oxidation process.

However, the two thiol dendrons **8** and **10** were fully characterized by analytical and spectroscopic techniques including the molecular peaks in their MALDI TOF mass spectra (see the experimental procedures in the Supporting Information).

B. AB_9 Dendrons. From the AB_3 unit **1**, two phenolic nona-allyl AB_9 dendrons were synthesized using convergent strategies (Scheme 2). The allyl branches of **1** were either hydroborated, and then oxidized to alcohol and transformed into iodo termini, or catalytically hydrosilylated by dimethylchloromethylsilane followed by halogen exchange for iodo. These two triodo derivatives were protected at the phenol focal point by reaction with propionyl iodide, which gave the protected triodo derivatives **13** and **14**. These two compounds reacted with **1** to give nona-allyl AB_9 units **15** and **16** after deprotection. These two phenol nona-allyl derivatives were hydrosilylated using ferrocenyldimethylsilane yielding **17** and **18**, then reaction of the phenol group with *p*.dibromoxylene gave the bromomethyl

(12) (a) Valério, C.; Fillaut, J.-L.; Ruiz, J.; Guittard, J.; Blais, J.-C.; Astruc, D. *J. Am. Chem. Soc.* **1997**, *119*, 2588. (b) Valério, C.; Alonso, E.; Ruiz, J.; Blais, J.-C.; Astruc, D. *Angew. Chem., Int. Ed.* **1999**, *38*, 1747. (c) Labande, A.; Astruc, D. *Chem. Commun*. **2000**, 1007. (d) Nlate, S.; Ruiz, J.; Sartor, V.; Navarro, R.; Blais, J.-C.; Astruc, D. *Chem.−Eur. J*. **2000**, *6*, 2544. (e) Labande, A.; Ruiz, J.; Astruc, D. *J. Am. Chem. Soc.* **2002**, *124*, 1782.
(13) Fitzmaurice, D.; Rao, S. N.; Preece, J.; Stoddart, J. F.; Wenger, S.; Zaccheroni, N. *Angew. Chem., Int. Ed.* **1999**, *38*, 1147.
(14) Sampath, S.; Lev, O. *Adv. Mater*. **1997**, *9*, 410.
(15) (a) Boal, A. K.; Rotello, V. M. *J. Am. Chem. Soc.* **1999**, *121*, 4914. (b) Boal, A. K.; Rotello, V. M. *J. Am. Chem. Soc.* **2000**, *122*, 734. (c) Niemz, A.; Rotello, V. M. *Acc. Chem. Res.* **1999**, *32*, 44.
(16) (a) Storhoff, J. J.; Elghanian, R.; Mucic, R. C.; Mirkin, C. A.; Letsinger, R. L. *J. Am. Chem. Soc.* **1998**, *120*, 1959. (b) Mucic, R. C.; Storhoff, J. J.; Mirkin, C. A.; Letsinger, R. L. *J. Am. Chem. Soc*. **1998**, *120*, 12674. (c) Elghanian, R.; Storhoff, J. J.; Mucic, R. C.; Letsinger, R. L.; Mirkin, C. A. *Science*, **1997**, *277*, 1078.
(17) Shenton, W.; Davis, D. A.; Mann, S. *Adv. Mater*. **1999**, *119*, 11132.
(18) (a) Weber, K.; Creager, S. E. *Anal. Chem.* **1994**, *66*, 3164. (b) Weber, K.; Hockett, L.; Creager, S. E. *J. Phys. Chem. B.* **1997**, *101*, 8286. (c) Hosteler, M. J.; Green, S. J.; Stockes, J. J.; Murray, R. W. *J. Am. Chem. Soc*. **1996**, *118*, 4212.
(19) (a) Horikoshi, T.; Itoh, M.; Kurihara, M.; Kubo, K.; Nishihara, H. *J. Electroanal. Chem*. **1999**, *473*, 113. (b) Yamada, M.; Tadera, T.; Kubo, K.; Nishihara, H. *Langmuir,* **2001**, *17*, 2263.
(20) (a) Brust, M.; Walker, M.; Bethell, D.; Schiffrin, D. J.; Whyman, R. *J. Chem. Soc., Chem. Commun.* **1994**, 801. (b) Brust, M.; Fink, J.; Bethell, D.; Schiffrin, D. J.; Kiely, C. *J. Chem. Soc., Chem. Commun.* **1995**, 1655.
(21) Sartor, V.; Djakovitch, L.; Fillaut, J.-L.; Moulines, F.; Neveu, F.; Marvaud, V.; Guittard, J.; Blais, J.-C.; Astruc, D. *J. Am. Chem. Soc.* **1999**, *121*, 2929. Sartor, V.; Nlate, S.; Djakovitch, L.; Fillaut, J.-L.; Moulines, F.; Neveu, F.; Marvaud, V.; Guittard, J.; Blais, J.-C.; Astruc, D. *New J. Chem*. **2000**, *24*, 351. Nlate, S.; Blais, J.-C.; Astruc, D. *New J. Chem*. **2003**, *27*, 178.
(22) Jutzi, P.; Batz, C.; Neumann, B.; Stammler, H. G. *Angew. Chem., Int. Ed. Engl.* **1996**, *35*, 2118.
(23) Krsda, S. W.; Seyferth, D. *J. Am. Chem. Soc.* **1998**, *120*, 3604.

Scheme 1. Synthesis of the AB_3 Thiol Ligands **8** and **10** Containing Ferrocenyl Groups

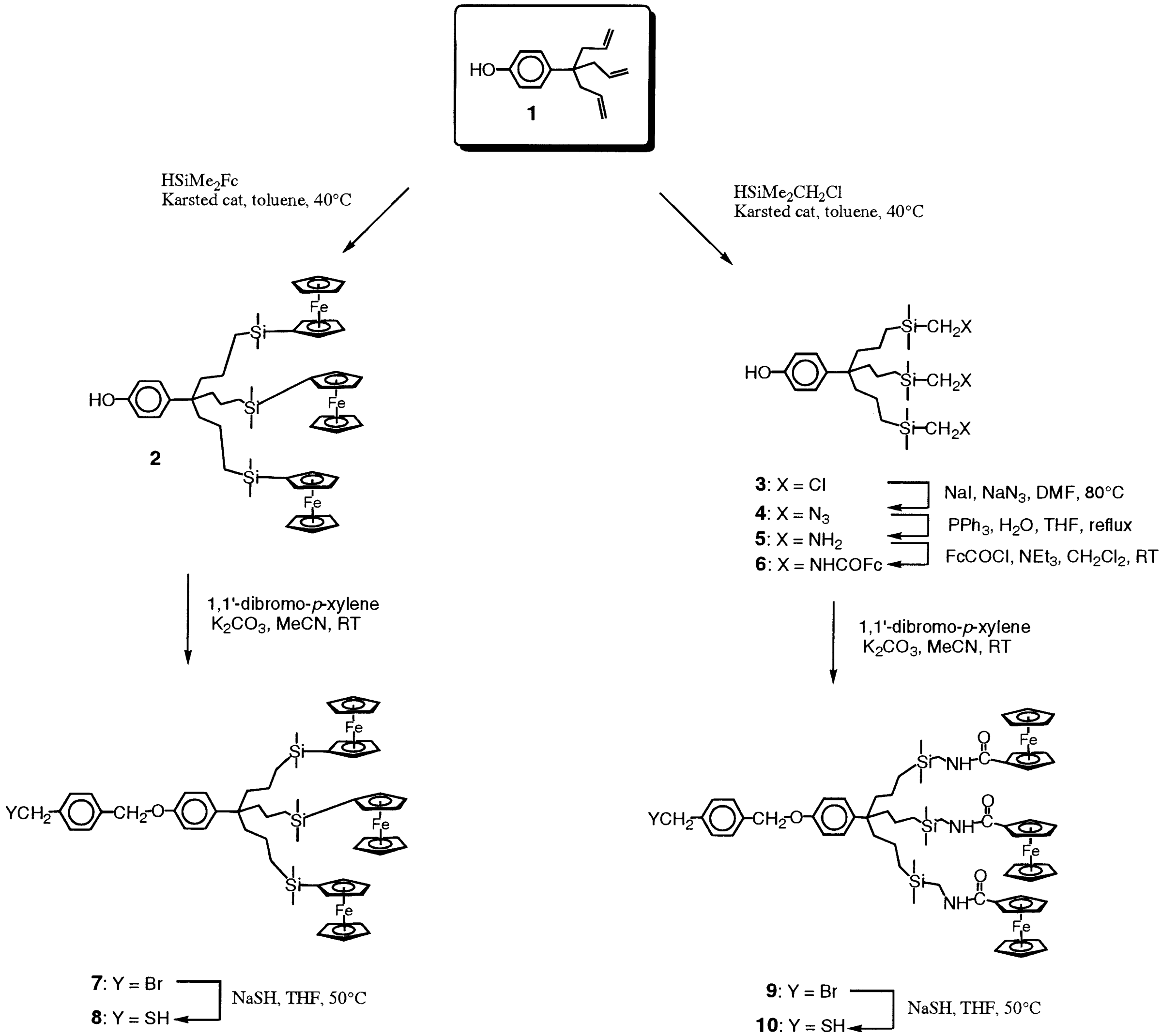

derivatives **19** and **20**, and finally substitution of Br^- by SH^- yielded the desired thiol dendrons **21** and **23**.

The AB_9 thiols **21** and **23** were fully characterized including by the prominent molecular peak in their MALDI TOF mass spectra. The thiol dendrons are air sensitive and show a strong tendency to oxidize to disulfide (see Scheme 3 where **21** is oxidized to **22**). Thus, reduction of the eventually partly oxidized thiols was systematically carried out just before dendron-colloid assembly in order to optimize the colloid yields whatever the type of colloid synthesis.

Colloid-Dendron Assemblies. Brust's method reproducibly leads to the synthesis of gold−dodecanethiolate particles of various sizes with narrow polydispersities,[20] and we chose to synthesize such colloids with a 2.3-nm diameter core and approximately 150 thiol ligands, which was checked by combined HRTEM and elemental analysis. Ligand-exchange reactions between these gold−dodecanethiolate particles and the thiol ligands **8** and **10** were carried out under ambient conditions in dichloromethane (Scheme 4). The functional thiol dendrons were used in excess (1 equiv of functional thiol *per* dodecanethiol ligand) leading to the dendron-functionalized particles **11** and **12**, and the excess of functional ligand was removed by washing **11** and **12** with methanol. The percentages of functional thiol dendrons introduced as ligands in **11** and **12**, determined by combined HRTEM (see the TEM pictures and histograms in the Supporting Information, Figures SI 1 to SI 4), ^{1}H NMR, and elemental analysis, were 4.8% and 3%, respectively. This corresponds, in average, to a little less than seven dendrons for **11** and five dendrons for **12**. The TEM pictures confirm that the sizes of the gold cores of the particles remain unchanged after the ligand-substitution reactions.

The limit of the ligand-substitution reaction was noted with larger dendrons. For instance, attempts to synthesize dendron-colloid assemblies using the nona-allyl dendron $HSCH_2p.C_6H_4$-$CH_2p.OC_6H_4C[C(CH_2)_3OC_6H_4C(CH_2CHCH_2)_3]_3$ resulted in the incorporation of very little dendron, that is, less than one per colloid particle. Under these conditions, reactions with even larger nonametallic dendrons containing nine ferrocenyl groups for recognition purpose appeared hopeless. Therefore, we embarked into a different strategy that consisted in carrying out direct Brust-type nanoparticle syntheses using mixtures of linear dodecanethiols and dendronized thiols containing nine ferrocenyl groups. The direct synthesis was first successfully attempted using the trisilylferrocenyl thiol which gave **11a**, whose characteristics turned out to be similar to those of the colloid **11** obtained by the previous ligand-substitution procedure. It was expected that linear dodecanethiol molecules would become thiolate ligands of gold particles more easily than the den-

Scheme 2. Synthesis of the Two Nonasilylferrocenyl Thiol Dendrons (AB_9 Units) **21** and **23** Starting from the Triallylphenol Molecular Brick **1**

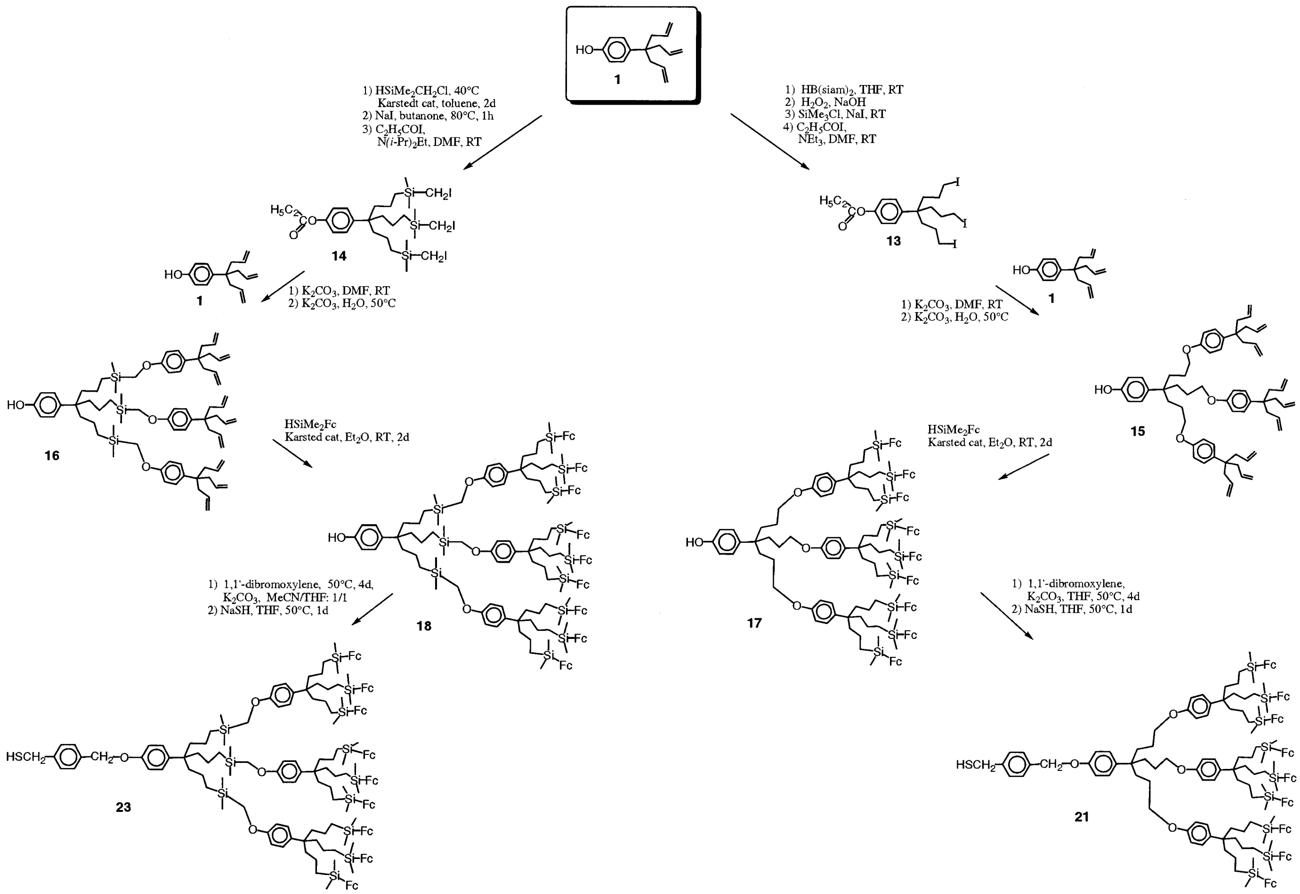

Scheme 3. Reversible Dimerization of the Nonaferrocenyl Thiol Dendrons upon Exposure to Air

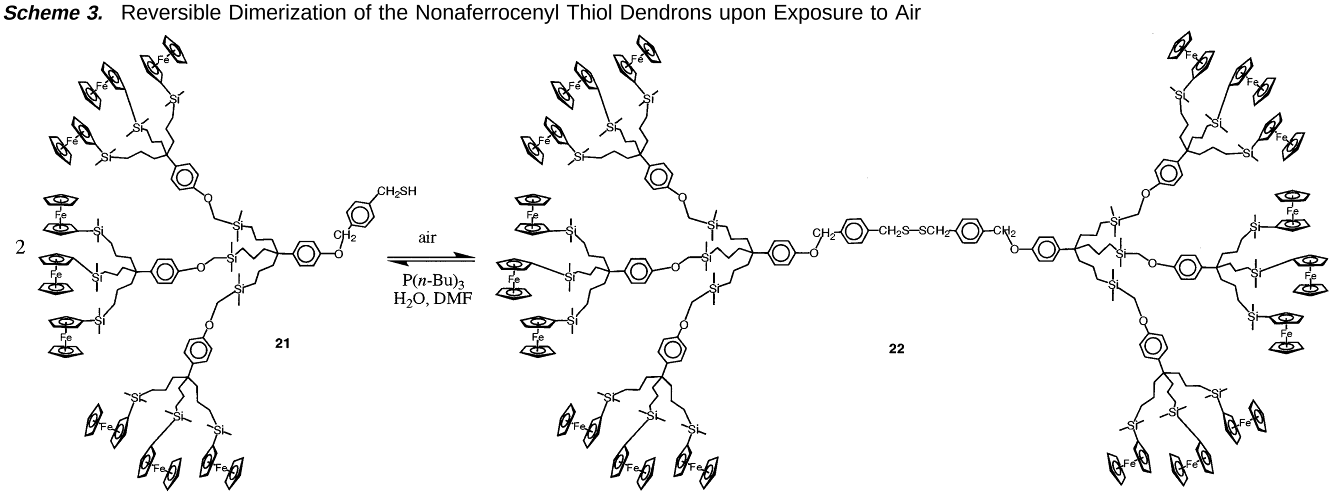

dronized thiols, especially with the bulky nonaferrocenylthiol dendrons. Indeed, their proportion found in the nanoparticles obtained was higher than that in the reaction mixture that systematically contained an equimolar ratio of both dodecanethiol and dendronized thiol. Nevertheless, this technique is very successful and allows efficient synthesis of colloids **24** and **25** with good amounts of nonaferrocenyl dendronized thiols (Schemes 5 and 6). Adjusting the proportion of ligands and gold source can control the size of the particles, although the particles made in this way are larger (2.9 nm diameter) than those synthesized by the substitution method. We first attempted it using the trisilyl dendron that could be introduced in a proportion of 25%. Then, the two nonaferrocenylthiol dendrons could form dendronized nanoparticles containing, respectively, 10 and 20% of dendrons among the thiol ligands. This means that, for a colloid of a 2.9-nm diameter bearing around 200 thiolate ligands, there are about 20 and 40, respectively, dendronized thiolates bearing around 180 and 360, respectively, ferrocenyl units linked to the colloidal core, which makes a rather bulky periphery. The cavities near the core, located between the particle surface and the ferrocenyl layer at the periphery, are filled with about 180 and 160, respectively, linear dodecanethiolate ligands, as schematically represented on Schemes 5 and 6. The proportions of dendronized and linear ligands in **24** and **25** were determined

Scheme 4. Synthesis of the Dendronized Gold Colloids **11** and **12** Using the Thiol-Ligand Substitution Procedure

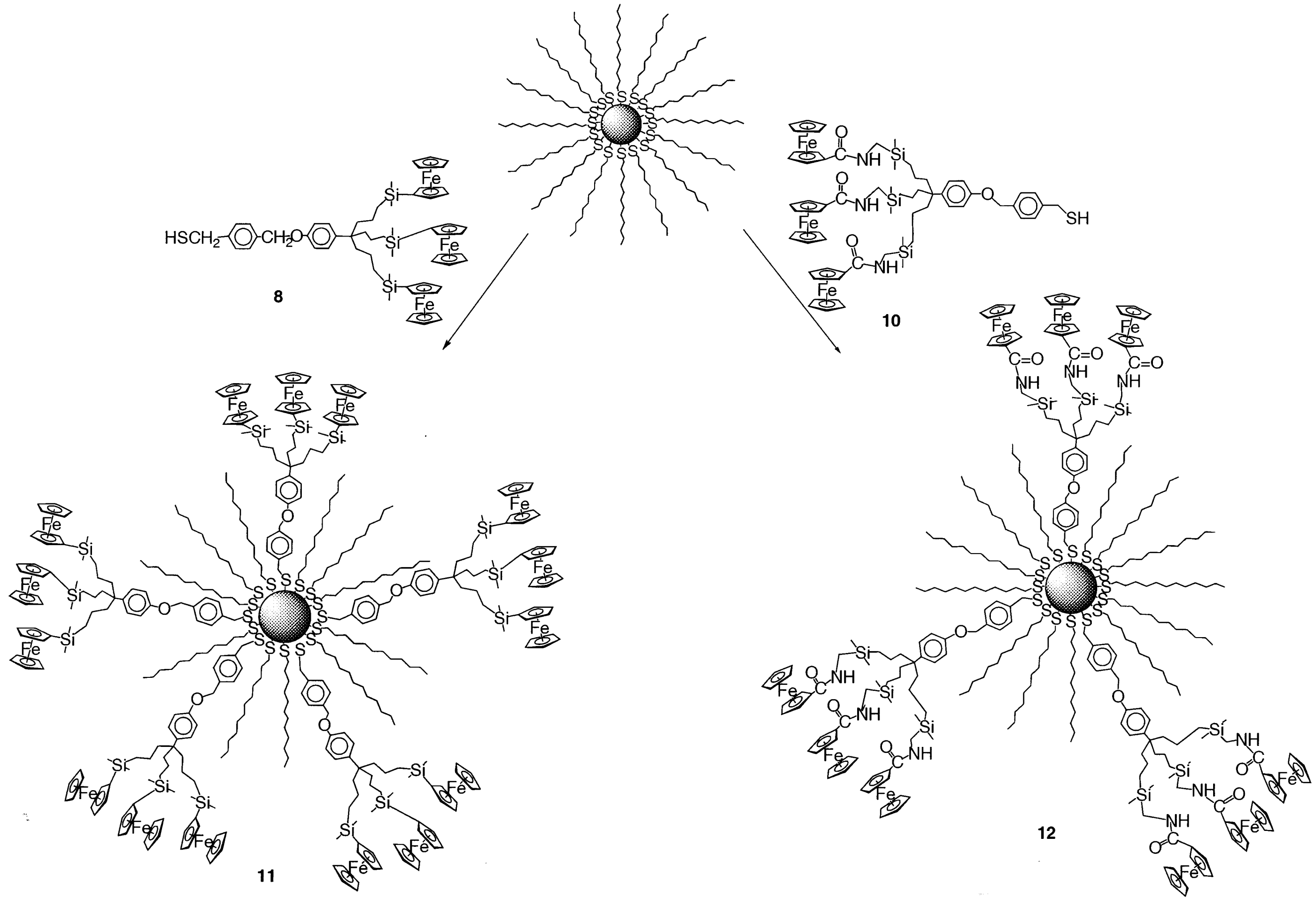

Scheme 5. Direct Synthesis of the Dendronized Gold Colloid **24** Containing the Nonaferrocenyl Thiol Dendron **21** (About 180 Ferrocenyl Groups)

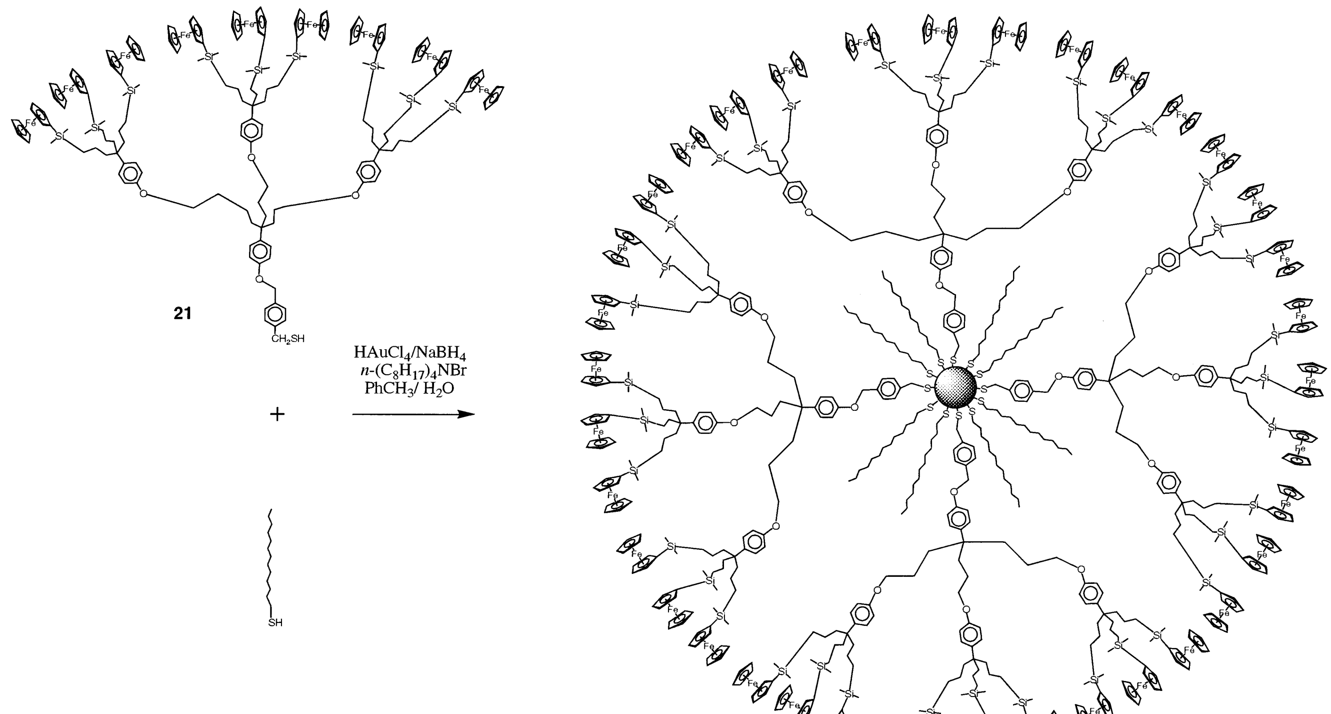

by integration of the respective ^{1}H NMR signals of these ligands and by electrochemical titration (vide infra).

Cyclic Voltammetry Studies of the Metallodendron-Colloid Assemblies. The cyclovoltammograms (CV) of the

Scheme 6. Direct Synthesis of Dendronized Gold Colloid **25** Containing the Nonaferrocenyl Thiol Dendron **23** (About 360 Ferrocenyl Groups)

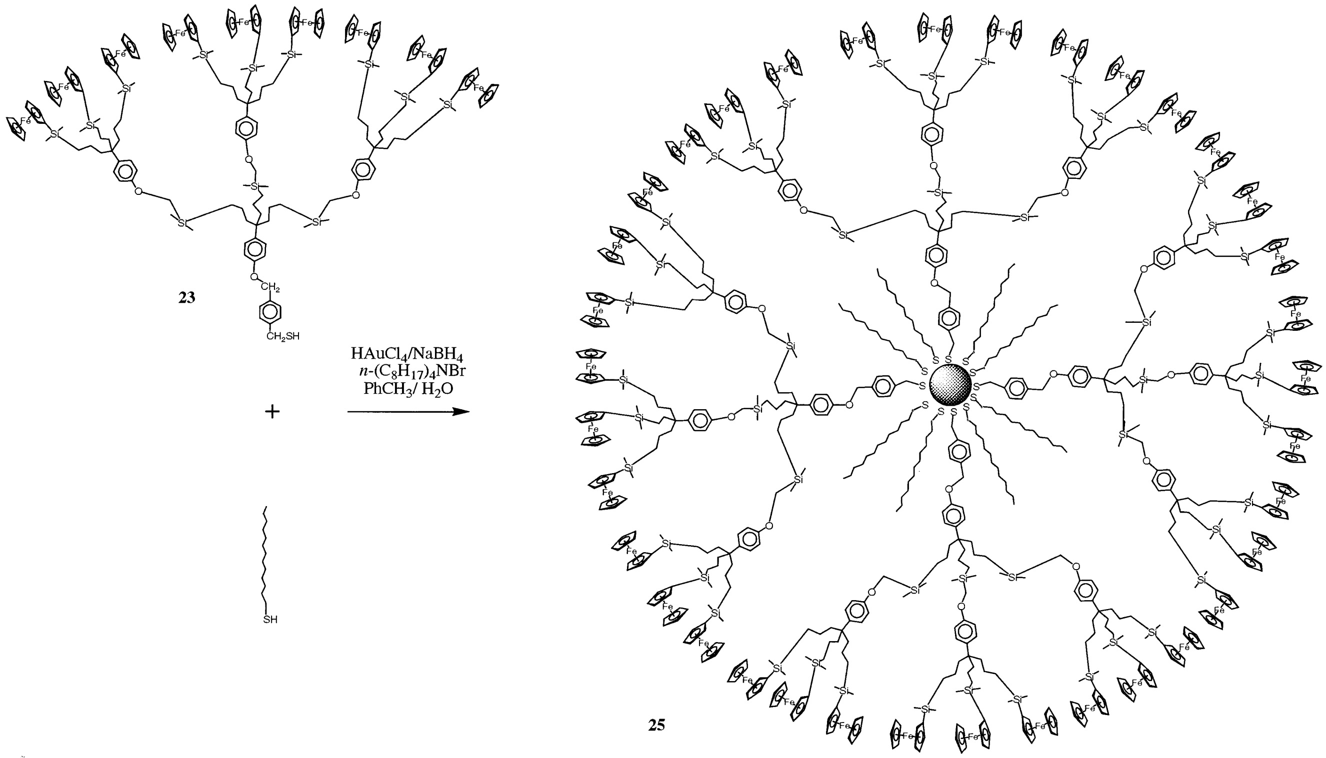

dendronized gold nanoparticles **11**, **12**, **24**, and **25** (Pt, CH_2Cl_2, 0.1 M $[NBu_4][PF_6]$) show a chemically (i_a/i_c = 1) and electrochemically ($\Delta E_p \leq$ 50 mV) reversible ferrocene/ferrocenium wave.[24-26] Although these waves look like single-electron waves, the total number of electrons exchanged per particles corresponds to the total number of ferrocenyl units per particle, that is, for instance about 30 for **11** and 18 for **12**. These numbers cannot be determined using the Bard−Anson formula,[24b] which is working well with polymers including dendrimers, however, contrary to what could be achieved with metallodendrimers,[12] because the gold core is too large and heavy. All the ferrocenyl units look equivalent, in each type of particle, which is due, in particular, to the fact that rotation of the particles is faster than the electrochemical time scale.[27] The separation between the anodic and cathodic peaks is 50 mV for **11** and **12**, which almost corresponds to the 58-mV value expected at 20 °C for a single-electron wave. Values lower than 58 mV indicate that some adsorption[27b,c] occurs, although this phenomenon is weak and not accompanied by an enhanced intensity of the adsorbed dendronized colloids alone (see Table 1).

The $E_{1/2}$ value is 0 V versus $Cp_2Fe^{0/+}$ for **11** and 0.145 V versus $Cp_2Fe^{0/+}$ for **12**.[25b] The dendronized colloids **24** and **25** containing the nonaferrocenyl dendrons adsorb more strongly than the colloids **11** and **12** that contain AB_3 units when the CV are recorded using CH_2Cl_2 solutions. This latter parameter can eventually influence the choices of conditions for the recognition experiments in solution or at modified electrodes (vide infra).

Recognition of $H_2PO_4^-$, HSO_4^-, and ATP^{2-}. (a) $H_2PO_4^-$. We have examined the interaction between $H_2PO_4^-$ and the new dendronized colloids by adding $[n\text{-}Bu_4N][H_2PO_4]$ to the electrochemical cell containing one of the dendronized colloids. This led to the decrease of the intensity of the ferrocenyl wave and to the concomitant appearance and growth of another wave at a less positive potential until the initial wave disappeared when the amount of $[n\text{-}Bu_4N][H_2PO_4]$ added corresponded to 1 equiv *per* amidoferrocenyl branch. Thus, the new wave corresponds to the interaction between $H_2PO_4^-$ and the branch containing the ferrocenyl group, and this appearance of a new wave is the signature of a strong interaction. This new wave, contrary to the initial one, shows the characteristic of a slow electron transfer, since the ΔE_p value is more or less larger than 60 mV and depends on the scan rate, meaning that some structural reorganization intervenes in the course of the heterogeneous electron transfer.[24,25] The value of $E_{1/2}$ for each wave does not vary during the titration. For instance, with the dendronized colloid **12** containing AB_3 units that bear three amidoferrocenyl groups, the difference remains equal to 210 ± 10 mV. Yet, in this particular case, the recognition is marred by the partial chemical irreversibility of the system in solution, contrary to

(24) (a) Bard, A. J.; Faulkner, L. R. *Electrochemical Methods*; Wiley: New York, 1980. (b) Flanagan, J. B; Margel, S.; Bard, A. J.; Anson, F. C. *J. Am. Chem. Soc*. **1978**, *100*, 4248.
(25) (a) Astruc, D. *Electron-Transfer and Radical Processes in Transition-Metal Chemistry;* VCH: New York, 1995; Chapters 2 and 7. (b) the internal reference was decamethylferrocene, $[FeCp^*_2]$, a much better reference than ferrocene (the $E°$ values are then converted vs $[FeCp_2]$, however). See: Ruiz, J.; Astruc, D. *C. R. Acad. Sci., Ser. IIc: Chim.* **1998**, 21. Astruc, D. In *Electron Transfer in Chemistry*; Balzani, V., Mattay, J., Astruc, D., Eds.; Vol. 2. Organic, Inorganic and Organometallic Molecules; Wiley-VCH: New York, 2001; section 2, Chapter 4, p 728.
(26) Kaifer, A E.; Gomez-Kaifer, M. *Supramolecular Electrochemistry*; Wiley-VCH: Weinheim, Germany, 1999; Chapter 16, p 207.
(27) (a) Gorman, C. B.; Smith, J. C.; Hager, M. W.; Parkhurst, B. L.; Sierzputowsska-Gracz, H.; Haney, C. A. *J. Am. Chem. Soc*. **1999**, *121*, 9958. (b) For the adsorption of organothiol dendrons on a gold surface, see: Gorman, C. B.; Miller, R. L.; Chen, K. Y.; Bishop, A. R.; Haasch, R. T.; Nuzzo, R. G. *Langmuir*, **1998**, *14*, 3312. (c) For a review on dendritic thin films and monolayers, see: Schenning, A. P. H. J.; Weener, J. W.; Meijers, E. W. In *Conjugated Polymers and Molecular Interfaces*; Salaneck, W. R. R., Seki, K., Kahn, A., Pireaux, J.-J., Eds.; Marcel Dekker: New York, 2001, p 1.

Table 1. Electrochemical Characteristics of the Dendronized Gold Colloids **11**, **12**, **24**, and **25** before and after Titration of the $H_2PO_4^-$ and ATP^{2-} Anions and of the Stable Modified Electrodes Obtained with Colloids **12**, **24**, and **25**

	$E_{1/2}$[a] ($E_{pa} - E_{pc}$)	i_{pc}/i_{pa}[b]	$E_{1/2initial} - E_{1/2new}$[c] with $H_2PO_4^-$	$K_{(+)}/K_{(0)}$[d]	$E_{1/2initial} - E_{1/2new}$[c] with ATP^{2-}	$K_{(+)}/K_{(0)}$[e]
colloid-3-amido-Fc **12**	0.680 (0.050)	1.0	0.200 (0.130)	2800 ± 600	0.170 (0.170)	850 ± 200
colloid-3-silyl-Fc **11**	0.545 (0.050)	1.0	0.115 (0.070)	96 ± 20	0.080 (0.070)	24 ± 5
colloid-3-silyl-Fc **24**	0.545 (0.025)	1.2	0.135 (0.060)	210 ± 40	0.100 (0.070)	53 ± 10
colloid-9-silyl-silyl-Fc **25**	0.545 (0.025)	1.2	0.125 (0.050)	140 ± 30	0.090 (0.050)	36 ± 7
modified Pt electrode with the colloid-3-amido-Fc **12**	0.680 (0.0) $\Delta E_{FWHM} = 0.100$[f]	1.0	0.160 (0.070) $\Delta E_{FWHM} = 0.150$	600 ± 100	0.175 (0.110) $\Delta E_{FWHM} = 0.150$	1040 ± 200
modified Pt electrode with the colloid-9-silyl-Fc **24**	0.530 (0.0) $\Delta E_{FWHM} = 0.060$	1.0	0.120 (0.070) $\Delta E_{FWHM} = 0.100$	120 ± 30	0.090 (0.050) $\Delta E_{FWHM} = 0.100$	36 ± 7
modified Pt electrode with the colloid-9-silyl-silyl-Fc **25**	0.540 (0.0) $\Delta E_{FWHM} = 0.060$	1.0	0.130 (0.040) $\Delta E_{FWHM} = 0.100$	170 ± 40	0.090 (0.060) $\Delta E_{FWHM} = 0.100$	36 ± 7

[a] $E_{1/2}$ vs $FeCp^*_2$; electrolyte, [n-Bu_4N][PF_6]; working electrode, Pt. [b] Intensity ratio i_{pc}/i_{pa}, whose unity value shows the chemical reversibility and lack of adsorption. [c] Difference of $E_{1/2}$ value between the initial wave and the new wave at half titration in order to observe and compare both waves (see Figures 1−3). [d] Ratio between the apparent association constants $K_{(+)}/K_{(0)}$ of the cationic and neutral forms with the $H_2PO_4^-$ anion. [e] Ibid with the ATP^{2-} anion. [f] Full width of potential at half-maximum.

the other dendronized colloids that bear silylferrocenyl groups. This corresponds to an apparent association constant K between the ferrocenium form of **12** and $H_2PO_4^-$ that is 4200 times larger than the same constant between the neutral form of **11** and $H_2PO_4^-$.[28] This ratio is very large compared to that with monomeric amidoferrocenes ($E_{1/2free} - E_{1/2bound} = 45$ mV) and even that with tripodal tris-amidoferrocenes ($E_{1/2\ free} - E_{1/2bound} = 110$ mV) and is about as large as that with a nona-amidoferrocene dendrimer.[12a] The recognition of $H_2PO_4^-$ is very selective. We have tested other anions (HSO_4^-, Cl^-, Br^-, NO_3^-) which did not provoke the appearance of a new wave or a significant shift of the ferrocenyl wave. In particular, it is noteworthy that the other oxo-anion HSO_4^- did not interact significantly, whereas it is recognized by amidoferrocene dendrimers and colloid **12**.[12a]

With the dendronized colloids **11** containing AB_3 units bearing three silylferrocenyl groups, the difference between the potentials $E_{1/2}$ of the initial and new waves is smaller (110 mV) than that with **12**. The chemical reversibility obtained under ambient condition, however, was encouraging to investigate further such silylferrocenyl systems with AB_9 dendrons and especially with electrodes modified with dendronized colloids bearing such large dendrons (vide infra). Gratifyingly, this difference of potentials appears to be somewhat larger with the two dendronized colloids bearing these AB_9 silylferrocenyl units, meaning that the recognition is subjected to a positive dendritic effect. The characteristics of the electrochemical recognition features by all the dendronized colloids are gathered in Table 1. The potential differences between the two waves show the magnitude of the recognition. The differences ΔE_p between the anodic and cathodic peaks of each wave indicate whether the heterogeneous electron transfer is fast ($\Delta E_p = 60$ mV) or slowed by the structural reorganization ($\Delta E_p > 60$ mV), especially during the increase of interaction with the anion upon oxidation of the ferrocenyl unit to ferrocenium. The intensity i_c/i_a ratio shows cases for which one is dealing with chemical irreversibility ($i_c/i_a < 1$) or adsorption ($i_c/i_a > 1$). The comparison between the colloid dendronized with the AB_3 units and those dendronized with the AB_9 units shows the advantage of the AB_9 dendronized colloid with silylferrocenyl groups disclosing a larger potential shift due to the positive dendritic effect (Figure SI 5). These two dendrons show identical characteristics for the recognition of these anions. Given these satisfactory redox recognition features, titration of [n-Bu_4N][H_2PO_4] can be carried out. The equivalence points of these titrations can be determined either from the decrease of intensity of the initial ferrocenyl wave or increase of intensity of the new ferrocenyl−$H_2PO_4^-$ wave at less positive potential. Both variations yield close results, and the data obtained also corresponded with 5−10% errors to the amount of redox active species. Indeed, this amount was also determined by integration of the ^1H NMR signals, in the dendrons coordinated to the colloidal core (assuming a one-to-one interaction of the ferrocenyl group with $H_2PO_4^-$ and two-to-one for ATP^{2-}). All the dendronized colloids gave satisfactory titration graphs (see all the titration graphs in the Supporting Information, Figures SI 7 to SI 15), since the separation between the initial and new wave is relatively large and the intensities are not much marred by adsorption in the beginning or during the titration.

(b) Adenosine-5′-triphosphate, ATP^{2-}. The addition of [n-Bu_4N]$_2$[ATP] to the electrochemical cell containing the dendronized colloid provokes the apparition of a new wave, just as with the [n-Bu_4N][H_2PO_4] salt. The potential difference between the initial and new wave is of the same order of magnitude with those of [n-Bu_4N]$_2$[ATP] and [n-Bu_4N][H_2PO_4] (slightly smaller for [Bu_4N]$_2$[ATP] than for [n-Bu_4N][H_2PO_4]) with all the dendronized colloids studied here. Table 1 also gathers the data of this recognition of [n-Bu_4N] $_2$[ATP] in the same fashion as for [n-Bu_4N][H_2PO_4]. Figure 1 shows the CVs in the course of the titrations; that is, both the initial and new waves are visible at this stage.

Thus, these waves can be compared for the tris-amidoferrocenyl-dendronized colloid **12** (Figure SI 6) and a nonaferrocenyl-dendronized colloid (good wave separation and chemical

(28) Reynes, O.; Moutet, J.-C.; Pecaut, J.; Royal, G.; Saint-Aman E. *Chem.*−*Eur*. J. **2000**, *6*, 2544.

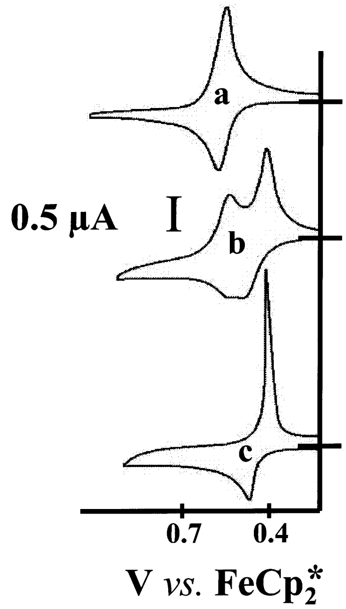

Figure 1. Titration of ATP^{2-} with **24** (colloid 9-silyl-Fc) in CH_2Cl_2. Cyclic voltammograms: electrolyte support, 0.1 M [n-Bu_4N][PF_6]; reference electrode, Ag; auxiliary and working electrodes, Pt; scan rate, 0.2 V/s; solution of [n-Bu_4N]$_2$[ATP], 5×10^{-3} M; internal reference, $FeCp_2$*. (a) nanoparticle alone; (b) in the course of the titration (note the two close waves on the cathodic side); (c) with an excess of [n-Bu_4N]$_2$[ATP].

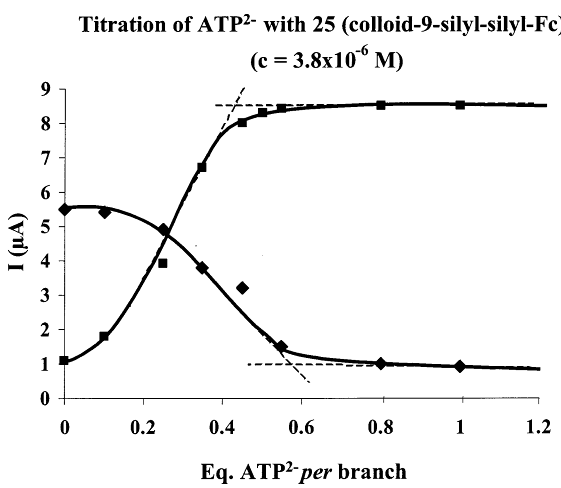

Figure 2. Titration of ATP^{2-} with **25** (colloid-9-silyl-silyl-Fc). Decrease of the intensity of the initial CV wave (◆) and increase of the intensity of the new CV wave (■) vs the number of equiv of [n-Bu_4N]$_2$[ATP] added per ferrocenyl branch. Nanoparticles: 3.8×10^{-6} M in CH_2Cl_2. See the caption to Figure 1 for the conditions.

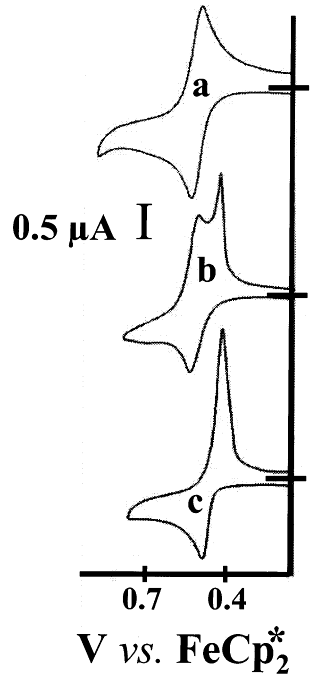

Figure 3. Titration of ATP^{2-} with **24** (colloid-9-silyl-Fc) in the presence of [n-Bu_4N][Cl] and [n-Bu_4N][HSO_4] (both anions, 5×10^{-2} M, 0.5 equiv *per* ferrocenyl branch): cyclic voltammograms (see Figure 1 for the experimental conditions). (a) nanoparticle **24** alone; (b) in the course of the titration; (c) with an excess of [n-Bu_4N]$_2$[ATP].

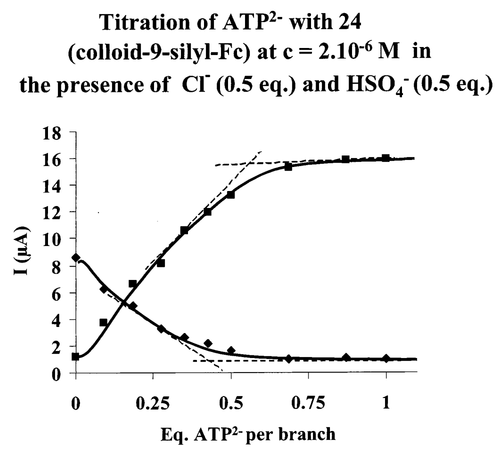

Figure 4. Titration of ATP^{2-} with **24** (colloid-9-silyl-Fc) in the presence of [n-Bu_4N][Cl] and [n-Bu_4N][HSO_4] (both anions, 0.5 equiv *per* ferrocenyl branch). Decrease of the intensity of the initial CV wave (◆) and increase of the intensity of the new CV wave (■) vs the number of equiv of [n-Bu_4N]$_2$[ATP] added per ferrocenyl branch. Nanoparticles: 2×10^{-6} M in CH_2Cl_2. See also Figure 1 for the conditions.

reversibility, Figure 1). A key difference between $H_2PO_4^-$ and ATP^{2-} resides in the stoichiometry obtained in the titration of ATP^{2-} that is half that of [n-Bu_4N][H_2PO_4] because of the double anionic charge of ATP^{2-}. This finding is not trivial, however, since recent ATP^{2-} titration with monoferrocenyl derivatives led to very different ATP^{2-} stoichiometries.[28] An example of CV obtained during ATP^{2-} titration with the colloid **24** dendronized with the AB_9 unit **21** is shown in Figure 1, whereas the corresponding titration graph is shown in Figure 2 for colloid **25**.

The selective recognition and titration of ATP^{2-} can also be carried out in the presence of [n-Bu_4N][Cl] and [n-Bu_4N][HSO_4] using colloid **24**. The addition of these latter salts to **24** does not provoke the appearance of a new CV wave or a shift of the initial CV wave. A new wave appears, upon addition of [n-Bu_4N]$_2$[ATP], only on the cathodic side at a potential 100 mV less positive than that of the initial wave. On the anodic side, the initial wave is progressively shifted until the equivalent point is reached, the total shift along the titration being 50 mV. These features are original. Figure 3 shows the CV before, during, and after titration, and Figure 4 shows the titration graph using the changes of intensities of the initial and new wave.

(c) HSO_4^-. The interaction of the silylferrocenyl-containing colloids **11**, **24**, and **25** with HSO_4^- is negligible, but recognition and titration can be carried out using the colloid **12** that bears the tris-amidoferrocenyl units. The latter provides a stronger interaction than those of the other colloids with HSO_4^-. The

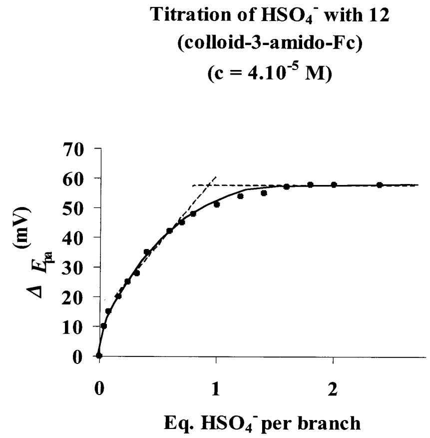

Figure 5. Titration of HSO_4^- with **12** (colloid-3-amido-Fc): shift of E_{pa} toward positive potentials recorded by CV as a function of the number of equiv [n-Bu_4N][HSO_4] added *per* amidoferrocenyl branch of the colloid. Nanoparticles: 4×10^{-5} M in CH_2Cl_2. See also Figure 1 for experimental conditions.

addition of [n-Bu_4N][HSO_4] to the electrochemical cell containing **12** does not provoke the apparition of a new CV wave, however, and only a shift of the CV wave is observed. The maximum shift of 60 mV for the anodic wave potential and 25 mV for the cathodic one are reached around the equivalent point, which allows titrating [n-Bu_4N][HSO_4], as shown in Figure 5. The absolute apparent association constant K^+ between **12** and the anion HSO_4^- is then defined by log $K^+c = \Delta E_{1/2}/0.058$[33] at 20 °C, giving $K^+ = (18 \pm 4) \times 10^3$ L mol^{-1}. The weaker interaction of the amidoferrocenyl group with HSO_4^- than that with $H_2PO_4^-$ has already been discussed.[12e] It is due to the fact that the negative charge density on the oxygen atoms is weaker in HSO_4^- than in $H_2PO_4^-$. The H bonding between these O atoms and the positively polarized nitrogen atom of the amido group dominates the overall H-bonding interaction. The silicon atom plays this role of the positively polarized nitrogen atom in the silylferrocenyl-branched dendrons because of the stabilization of a positive charge in the β position relative to the metal. This difference in H-bonding abilities of the functional ferrocenyl branch with HSO_4^- and H_2PO_4 is seemingly responsible for the observed selectivity.

Modified Electrodes. Electrodes modified by polymers containing ferrocenyl units have been known for a long time.[29] More recently, Cuadrado et al. have extensively studied the derivatization of silylferrocenyl-terminated and other ferrocenyl dendrimers.[30,31] The only report of modified electrodes with thiol−gold colloid assemblies functionalized by ferrocenyl dendrimers, however, is that of Nishihara's group.[32] To test the possible applications of dendronized colloids, we attempted to modify platinum electrodes by depositing these polyferrocenyl dendronized colloids. Previous attempts to do so with amidoferrocenylalkylthiol−gold colloids that were recently reported met with failure, because they resulted in unstable modified electrodes. Nishihara has prepared modified electrodes with alkylthiol−gold colloids terminated by biferrocenyl units that may be considered as AB_2 units.[32] The seminal works of Crooks and Tomalia, who prepared dendrimer-colloid assemblies, showed that such assemblies are stable.[1] In the previous electrochemical study of the polyferrocenyl dendronized gold colloids, we could note the tendency of these nanoscopic assemblies to adsorb on electrodes. Indeed, we found that the adsorption of the dendronized gold colloids was all the better, as the thiols contained a larger number of ferrocenyl groups. The dendronized colloids bearing three ferrocenyl groups in AB_3 units adsorb better than monoferrocenylalkylthiols and allow preparing modestly stable electrodes. In this respect, the tris-amidoferrocenyl branching was found to give better results than the tri-silylferrocenyl one. The most stable modified electrodes were those prepared with the dendronized gold colloids containing either of the nonaferrocenyl dendrons. Indeed, the dendronized colloids containing the nonasilylferrocenylthiolate dendron give excellent modified electrodes, whereas the intensities and stabilities observed with those containing the trisilylferrocenylthiolate dendron are much weaker. These modified electrodes were prepared by simply dipping a platinum electrode into a CH_2Cl_2 solution of the dendronized colloid and scanning the potential back and forth around the ferrocenyl wave. This scanning provoked the appearance of the classic symmetric CV wave with the same anodic and cathodic potential disclosing an increase of its current intensity until saturation was reached after about fifty scans. These modified electrodes were perfectly stable (including in air), and they also showed a remarkable change when the $H_2PO_4^-$ or ATP^{2-} anion was introduced into the CH_2Cl_2 solution. Figure 6 shows the progress of the CV waves from the initial one to the new one.

The new wave seen in the presence of one of these anions is largely shifted to a less positive potential as noted for the dendronized colloids in solution (see the potential shifts in Table 1 for the modified electrodes with the various dendronized colloids). The anodic and cathodic peak potentials are no longer identical; this indicates electrochemical irreversibility, that is, strong structural rearrangement due to the supramolecular interactions (hydrogen bonding and especially electrostatic interaction) in the course of electron transfer. Remarkable features were the following:

(i) The stability of these CV waves upon multiple scanning the potentials around the waves.

(ii) The selective recognition of $H_2PO_4^-$ or ATP^{2-} in the presence of other anions, such as HSO_4^- and Cl^-.

(iii) The possibility to selectively wash the salts from these modified electrodes, leaving only the dendronized colloid on the electrode surface (Figure 6d). This allowed sensing this anion again in another solution or another anion. These experiments

(29) (a) Brown, A. P.; Anson, F. C. *Anal. Chem.* **1977**, *49*, 1589. (b) Peerce, P. J.; Bard, A. J. *Electroanal. Chem.* **1980**, *114*, 89. (c) Laviron, E. *J. Electroanal. Chem.* **1981**, *122*, 37. (d) Abruna, H. D. In *Electroresponsive Molecular and Polymeric Systems*; Stotheim, T. A., Ed.; Dekker: New York, 1988; Vol. 1, p 97. (e) Murray, R. W. In *Molecular Design of Electrode Surfaces*; Murray, R. W., Ed.; Techniques of Chemistry XXII; Wiley: New York, 1992; p 1. (f) Morán, M.; Casado, C. M.; Cuadrado, I. *Organometallics* **1993**, *12*, 4327. (g) Audebert, P.; Cerveau, G.; Corriu, R. J. P.; Costa, N. *J. Electroanal. Chem.* **1996**, *413*, 89.

(30) (a) Alonso, B.; Morán, M.; Casado, C.; Lobete, F.; Losada, J.; Cuadrado, I. *Chem. Mat.* **1995**, *7*, 1440. (b) Cuadrado, I.; Morán, M.; Losada, J.; Casado, M.; Pascual, C.; Alonso, B.; Lobete, F. In *Advances in Dendritic Macromolecules*; Newkome, G., Ed.; Jai Press: Stanford, CT, 1996; Vol. 3, p 151. (c) Cuadrado, I.; Casado, M.; Alonso, B.; Morán, M.; Losada, J.; Belsky, V. *J. Am. Chem. Soc.* **1997**, *119*, 7673.

(31) Reviews on ferrocenyl dendrimers and their electrochemistry:(a) Cuadrado, I.; Morán, M.; Casado, C. M.; Alonso, B.; Losada, J. *Coord. Chem. Rev.* **1999**, *193−195*, 395−445. (b) Casado, C. M.; Cuadrado, I.; Morán, M.; Alonso, B.; Garcia, B.; Gonzales, B.; Losada, J. *Coord. Chem. Rev.* **1999**, *185−186*, 53.

(32) (a) Biferrocenyl-substituted thiol-nanoparticles deposited on metal surfaces: Yamada, M.; Quiros, I.; Mizutani, J.; Kubo, K.; Nishihara, I. *Phys. Chem. Chem. Phys.* **2001**, *3*, 3377. (b) Yamada, M.; Kuzume, A.; Kurihara, M.; Kubo, K.; Nishihara, H. *Chem. Commun.* **2001**, 2476. (c) Yamada, M.; Nishihara, H. *Chem. Commun.* **2002**, 2578.

(33) Miller, S. R.; Gustowski, D. A.; Chen, Z.-H.; Gokel, G. W.; Echegoyen, L.; Kaifer, A. E. *Anal. Chem.* **1988**, *60*, 2021.

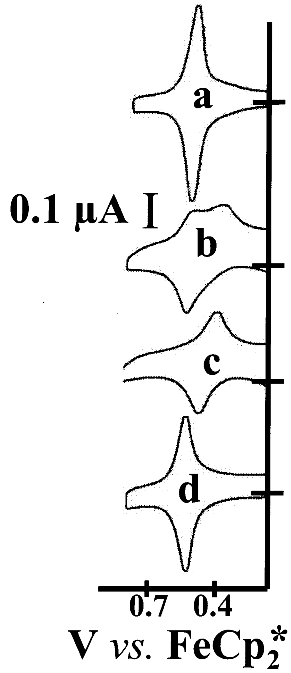

Figure 6. Recognition of ATP^{2-} with a Pt electrode modified: with 24 (colloid 9-silyl-Fc). Cyclic voltammograms: (a) 24-modified electrode alone; (b) in the course of the titration; (c) with an excess of $[n\text{-}Bu_4N]_2[ATP]$; (d) after removing ATP^{2-} by washing the 24-modified electrode with CH_2Cl_2. See experimental conditions in the caption to Figure 1.

show that adsorption is very strong upon scanning around the ferrocenyl potential area with such dendronized colloids loaded with a large number of ferrocenyl units, a feature that is very profitable for practical use of such modified electrodes.

Finally, the Pt electrode modified with **12** is also rather stable with a larger full width at half-maximun (100 mV) larger than the 90 mV value above which the adsorbed sites exert repulsive interactions among one another. This modified electrode also recognizes HSO_4^-, the potential being also shifted by 60 mV at the anode and by 25 mV at the cathode upon addition of this anion in solution (vide supra), which makes the signal slightly disymmetrical. As with $H_2PO_4^-$ and ATP^2, the modified electrode can be rinsed with CH_2Cl_2, after recognition of HSO_4^-, with minimal loss of adsorbed colloid for reuse. After using and washing 5 times, half the adsorbed redox active species is left, but further cycling and washing does not modify this amount any longer; the modified electrode is then stable.

Concluding Remarks

(a) Gold nanoparticles have been synthesized with both dodecanethiolate and the dendronized thiolate that contained triferrocenyl or nonaferrocenyl units either by the ligand-substitution procedure (AB_3 units) or by direct synthesis from mixtures of functional and nonfunctional thiols (AB_9 dendrons). The latter route is remarkably efficient for the nanoparticle−nonaferrocenyl dendronized assemblies when the substitution procedure is marred by the steric inhibition with large dendrons. With a gold nanoparticle−nonaferrocenylthiolate assembly, the colloidal gold core is surrounded by 180 or 360 silylferrocenyl units, so that these assemblies closely resemble large metallo-dendrimers in which the core is the gold nanoparticle.

(b) These dendronized gold nanoparticles combine the advantages of dendrimers and gold nanoparticles as sensors for the selective recognition and titration of $H_2PO_4^-$ and ATP^{2-} anions even in the presence of other anions. Their recognition properties are the subject of dendritic effect; that is, the shift of the ferrocenyl redox potential observed upon introduction of the anion is larger as the generation number increases. The assembly around the core provoking the clusterification of a large number of peripheral ferrocenyl groups induces the formation of narrow channels that facilitate the appearance of microcavities at the dendritic surface for a tighter supramolecular interaction with the anion. The silylferrocenyl system presents the advantage, over the amidoferrocenyl one, that its oxidation is fully reversible, although the provoked shift by addition of an anion is slightly larger with the amido group than with the silyl group. Although structural and electronic variations were designed concerning the size of the tethers and the number of Lewis-acidic silicon atoms in the dendrons **21** and **23**, the colloids **24** and **25** obtained with these two dendrons give similar recognition properties.

(c) The fabrication of modified electrodes is very successful only with the dendronized nanoparticles that contain the triamidoferrocenyl and nonaferrocenyl dendrons. This specific property cannot be obtained with the linear thiolate ligands and only begins to appear more or less weakly with the nanoparticles dendronized by the thiolate ligand containing the trisilylferrocenyl units. These modified electrodes recognize the $H_2PO_4^-$ and ATP^{2-} anions even in the presence of other anions such as HSO_4^- and Cl^-. HSO_4^- can also be recognized. Moreover, the salt of these anions can be easily removed after rinsing simply by dipping the used electrode a few minutes in CH_2Cl_2. In this way, the modified electrode with either of the dendronized nanoparticles can be reused many times.

Experimental Section

The synthesis of the AB_3 units from **1** is described in the Supporting Information. The preparation of the organic intermediates **13**−**17** was carried out as reported in ref 21.

Dendron 18. Karstedt catalyst (250 μL) was added to a mixture of nona-allyl dendron **16** (0.5 g, 0.44 mmol) and ferrocenyldimethylsilane (1.5 g, 6 mmol) in Et_2O, and this reaction mixture was stirred for 4 days at ambient temperature. The solution was filtered on Celite, and the solvent was removed under vacuum. After chromatographic separation on silica gel using a pentane/Et_2O (95:5) mixture as eluent, dendron **18** was obtained as an orange oil (1.2 g, 83%). Elemental analysis calcd for $C_{181}H_{248}Si_{12}Fe_9O_4$: H, 7.51; C, 65.33. Found: H, 7.59; C, 65.11. MALDI TOF mass spectrum, *m/z*: 3327.08 $[M]^+$ (calcd 3327.60). ^1H NMR ($CDCl_3$): δ_{ppm} 7.20 (d, C_6H_4, 6H); 7.09 (d, C_6H_4, 2H); 6.87 (d, C_6H_4, 6H); 6.67 (d, C_6H_4, 2H); 4.30 (s, C_5H_4, 2H); 4.09 (s, C_5H_5, 5H); 4.02 (s, C_5H_4, 2H); 3.51 (s, CH_2O, 6H); 1.61 (m broad, CH_2, 18H); 1.14 (m broad, CH_2, 18H); 0.62 (m broad, CH_2, 18H); 0.17 (s, SiMe, 54H); 0.08 (s, SiMe, 18H). ^{13}C NMR ($CDCl_3$): δ_{ppm} 159.38 (C_q, ArO); 152.84 (C_q, ArO); 139.77 (C_q, Ar); 137.17 (C_q, Ar); 127.51 (CH_{Ar}); 127.40 (CH_{Ar}); 114.65 (CH_{Ar}); 113.52 (CH_{Ar}); 73.04 (C_5H_4); 72.91 (C_q, C_5H_4); 70.69 (C_5H_4); 68.17 (C_5H_5); 60.09 (CH_2O); 43.13 (C_q−CH_2); 41.96 (CH_2); 17.90 (CH_2); 17.40 (CH_2Si); 14.58 (CH_2); −2.05 (SiMe); − 4.61 (SiMe).

Dendron 20. A mixture of **18** (0.600 g, 0.180 mmol), K_2CO_3 (0.076 g, 0.540 mmol), and 4, 4′-dibromomethylbenzene (0.476 g, 0.900 mmol) in CH_3CN/THF (50:50) was stirred for 4 days at 50 °C. After removal of the solvent under vacuum, the product was extracted with 3 × 30 mL of Et_2O, and the solvent was removed under vacuum. The residue was chromatographed on silica gel using a pentane/ether mixture (20:80) as eluent, and **20** was obtained as a yellow oil (0.600 g, 95%). Elemental analysis calcd for $C_{189}H_{255}O_4Si_{12}BrFe_9$: H, 7.32; C, 64.66. Found: H, 7.50; C, 64.33. MALDI TOF mass spectrum, *m/z*: 3510.07 $[M^+]$ (calcd 3510.65). ^1H NMR ($CDCl_3$): δ_{ppm} 7.38 (s, C_6H_4, 4H); 7.18

(d, C_6H_4, 10H); 6.86 (d, C_6H_4, 10H); 5.04 (s, OCH_2, 2H); 4.51 (s, BrCH_2, 2H); 4.31 (s, C_5H_4, 18H); 4.18 (s, C_5H_5, 45H); 4.02 (s, C_5H_4, 18H); 1.61 (m broad, CH_2, 18H); 1.14 (m broad, CH_2, 18H); 0.62 (m broad, CH_2, 18H); 0.17 (s, SiMe, 54H); 0.08 (s, SiMe, 18H). ^{13}C NMR ($CDCl_3$): δ_{ppm} 159.30 (C_q, ArO); 156.84 (C_q, ArO); 139. 70 (C_q, Ar); 137. 17 (C_q, Ar); 130.60 (C_q, Ar); 129.10 (C_q, Ar); 128.60 (CH_{Ar}); 127.40 (CH_{Ar}); 127.10 (CH_{Ar}); 114.65 (CH_{Ar}); 113.50 (CH_{Ar}); 72.97 (C_5H_4); 71.44 (C_q, C_5H_4); 70.62 (C_5H_4); 68.13 (C_5H_5); 66.10 (CH_2O); 60.09 (CH_2O); 43.13 (C_q-CH_2); 42.22 (CH_2); 33.09 (CH_2Br); 18.11 (CH_2); 17.59 (CH_2Si); 15.18 (CH_2); −1.85 (SiMe); −4.50 (SiMe).

Dendron 19. A mixture of **17** (0.500 g, 0.160 mmol), K_2CO_3 (0.045 g, 0.320 mmol), and 4,4′-dibromomethylbenzene (0.211 g, 0.800 mmol) in a CH_3CN was stirred for 4 days at 50 °C. After removal of the solvent under vacuum, the product was extracted with 2 × 20 mL of Et_2O. The solvent was removed in a vacuum. After chromatographic separation on silica gel using a pentane/ether mixture (20:80) as eluent, the bromobenzyl derivative **19** was obtained as a yellow oil (0.406 g, 77%). Elemental analysis calcd for $C_{180}H_{231}O_4Si_9BrFe_9$: H, 7.07; C, 65.63. Found: H, 7.51; C, 66.32. MALDI TOF mass spectrum, *m*/*z*: 3294.64 [M$^+$] (calcd 3294.11). ^{1}H NMR ($CDCl_3$): δ_{ppm} 7.42 (s, C_6H_4, 4H); 7.15 (d, C_6H_4, 10H); 6.80 (d, C_6H_4, 10H); 5.04 (s, OCH_2, 2H); 4.51 (s, BrCH_2, 2H); 4.30 (s, C_5H_4, 18H); 4.08 (s, C_5H_5, 45H); 4.01(s, C_5H_4, 18H); 3.87 (s, OCH_2, 6H); 1.61 (m broad, CH_2, 18H); 1.11 (m broad, CH_2, 18H); 0.59 (m broad, CH_2, 18H); 0.15 (s, SiMe, 54H). ^{13}C NMR ($CDCl_3$): δ_{ppm} 156.50 (C_q, ArO); 156.42 (C_q, ArO); 139.74 (C_q, Ar); 138.90 (C_q, Ar); 130.82 (C_q, Ar); 129. 19 (C_q, Ar); 128.73 (CH_{Ar}); 127.82 (CH_{Ar}); 127.28 (CH_{Ar}); 114.27 (CH_{Ar}); 113.55 (CH_{Ar}); 72.92 (C_5H_4); 71.40 (C_q, C_5H_4); 70.57 (C_5H_4); 68.20 (C_5H_5); 68.09 (CH_2O); 60.10 (CH_2O); 43.07 (C_q-CH_2); 42.04 (CH_2); 33.13 (CH_2-Br); 29.60 (CH_2); 17.95 (CH_2); 17.41 (CH_2Si); −2.03 (SiMe).

Dendron 21. A mixture of **19** (0.396 g, 0.120 mmol) and NaSH (0.068 g, 1.200 mmol) in THF was stirred for 24 h at 50 °C. After removal of the solvent under vacuum, the reaction product was extracted with 2 × 20 mL of Et_2O and chromatographed on a silica column using Et_2O, providing **21** as a yellow-orange oil (0.370 mg, 0.114 mmol, 95%). Elemental analysis calcd for $C_{180}H_{232}O_4Si_9Fe_9S$: H, 7.20; C, 66.58. Found: H, 7.61; C, 66.91. MALDI TOF mass spectrum, *m*/*z*: 3247.27 [M$^+$] (calcd 3445.60). ^{1}H NMR ($CDCl_3$): δ_{ppm} 7.38 (s, C_6H_4, 4H); 7.15 (d, C_6H_4, 8H); 6.69 (d, C_6H_4, 8H); 5.01 (s, OCH_2, 2H); 4.29 (s, C_5H_4, 2H); 4.08 (s, C_5H_5, 5H); 4.01 (s, C_5H_4, 2H); 3.87 (s, OCH_2, 6H); 3.60 (d, HSCH_2, 2H); 1.60 (m, CH_2, 18H); 1.13 (m, CH_2, 18H); 0.60 (m, CH_2, 18H); 0.16 (s, SiCH_3, 54H). ^{13}C NMR ($CDCl_3$): δ_{ppm} 156.70 (C_q, ArO); 156.42 (C_q, ArO); 139.74 (C_q, Ar); 138.90 (C_q, Ar); 130.80 (C_q, Ar); 129. 20 (C_q, Ar); 128.70 (CH_{Ar}); 127.82 (CH_{Ar}); 127.28 (CH_{Ar}); 114.26 (CH_{Ar}); 113.55 (CH_{Ar}); 73.04 (C_5H_4); 71.43 (C_q, C_5H_4); 70.70 (C_5H_4); 68.21 (C_5H_5); 66.01 (CH_2O); 60.10 (CH_2O); 43.05 (C_q-CH_2); 42.00 (CH_2); 35.50 ($HSCH_2$); 29.60 (CH_2); 17.95 (CH_2); 17.41 (CH_2Si); −1.88 (SiMe).

Reduction of Disulfides to Thiols. The dendron **21** oxidized by air to disulfide **22** (250 mg, 0.038 mmol) was dissolved with 10 mL of DMF in a Schlenk flask. Water (70 μL, 100 equiv) was added, then the reaction mixture was degassed, tris-*n*-butylphosphine (100 μL, 10 equiv) was introduced, and the mixture was stirred at room temperature for 3 h. Then, 50 mL of ethyl acetate was added, and the mixture was washed with 1 N HCl. The organic layer was separated, degassed, dried under Na_2SO_4, and filtered. The solvent was then removed under vacuum, and the solid residue was rinsed under positive nitrogen pressure using degassed petroleum ether. The orange solid thiol **21** (220 mg, 0.067 mmol, 88%) was dried under vacuum. The same procedure was applied to all the thiol dendrons just before the synthesis of dendronized nanoparticles.

Dendron 23. A mixture of **20** (0.300 g, 0.085 mmol) and NaSH (0.048 g, 0.854 mmol) in THF was stirred for 24 h at 50 °C. After removal of the solvent under vacuum, the reaction product was extracted with 2 × 20 mL Et_2O and chromatographed on a silica column using a pentane/Et_2O (90:10) mixture, providing **23** as a yellow-orange oil (0.277 mg, 0.080 mmol, 94%). Elemental analysis calcd for $C_{189}H_{256}O_4$-$Si_{12}Fe_9S$: H, 7.45; C, 65.54. Found: H, 7.88; C, 65.90. MALDI TOF mass spectrum, *m*/*z*: 3463.66 [M$^+$] (calcd 3463.81); 6927.21 [2M$^+$] (calcd 3927.62). ^{1}H NMR ($CDCl_3$): δ_{ppm} 7.38 (s, C_6H_4, 4H); 7.18 (d, C_6H_4, 8H); 6.87 (d, C_6H_4, 8H); 5.01 (s, OCH_2, 2H); 4.29 (s, C_5H_4, 2H); 4.08 (s, C_5H_5, 5H); 4.01 (s, C_5H_4, 2H); 3.60 (d, HSCH_2, 2H); 3.51 (s, OCH_2, 6H); 1.59 (m, CH_2, 18H); 1.13 (m, CH_2, 18H); 0.61 (m, CH_2, 18H); 0.16 (s, SiCH_3, 54H); 0.07 (s, SiCH_3, 18H). ^{13}C NMR ($CDCl_3$): δ_{ppm} 158.86 (C_q, ArO); 156.60 (C_q, ArO); 140.30 (C_q, Ar); 138.10 (C_q, Ar); 136.53 (C_q, Ar); 129.23 (C_q, Ar); 127.75 (CH_{Ar}); 127.10 (CH_{Ar}); 113.29 (CH_{Ar}); 72.95 (C_5H_4); 71.43 (C_q, C_5H_4); 70.60 (C_5H_4); 68.11 (C_5H_5); 66.11 (CH_2O); 60.10 (CH_2O); 43.04 (C_q-CH_2); 42.07 (CH_2); 35.50 ($HSCH_2$); 17.96 (CH_2); 15.18 (CH_2); −2.02 (SiMe); −4.64 (SiMe).

Ligand Substitution in Alkylthiol−Gold Nanoparticles. A CH_2Cl_2 (20 mL) solution of alkylthiol−gold nanoparticles (0.080 g, 10^{-6} mmol) and tris-ferrocenyl thiol dendron (see amounts later) was stirred under positive nitrogen pressure at room temperature. After 3 days, the solvent was evaporated under reduced pressure. The dark brown product was washed 3 times with 10 mL of methanol and then 3 times with 10 mL of acetone in order to remove the noncoordinated thiols, the desired colloids being not soluble in these two solvents (the washing solvents were finally colorless). The black solid was dried under vacuum.

(a) Dendron 11 (0.080 g, 0.073 mmol) gives 0.065 g of **11** (85% yield) and 4.8% of substitution in alkylthiol−gold nanoparticles. ^{1}H NMR (250 MHz, $CDCl_3$) δ_{ppm}: 7.33 (CH($C_6H_4CH_2S$)); 7.21 (CH-(C_6H_4O)); 6.91 (CH(C_6H_4O)); 4.94 (CH_2O); 4.31 (CH(C_5H_4Si)); 4.10 (Cp); 4.03 (CH(C_5H_4Si); 3.51 (SCH_2−arom.); 1.27 (CH_2 alkylthiol); 0.89 (CH_3 alkylthiol); 0.62 (CH_2Si); 0.08 (CH_3Si). ^{13}C NMR (62.9 MHz, $CDCl_3$) δ_{ppm}: 156.41 (C(C_6H_4O)); 142.13 (C($SCH_2(C_6H_4)CH_2$); 133.01 (CH($C_6H_4CH_2S$)); 132.3 (CH(C_6H_4O)); 112.4 (CH(C_6H_4O)); 72.5 (CH-(C_5H_4Si)); 70.5 (CH(C_5H_4Si)); 69.6 (CH(Cp)); 63.8 (CH_2O); 31.90−29.4 (CH_2 alkylthiol); 28.82 (SCH−arom.); 22.56 (CH_2 alkylthiol); 17.92 (CH_2C−arom.); 15.23 (CH_2CH_2Si); 14.1 (CH_3 alkylthiol); 3.11 (CH_2CH_2Si); −4.0 (CH_3Si). $E_{1/2}$ (V vs Fc; CH_2Cl_2; 20 °C) 0.00 (r) (see text).

(b) Dendron 12. (0.080 g, 0.063 mmol) gives 0.073 g of **12** (90% yield) and 3% of ligand substitution in alkylthiol−gold nanoparticles. ^{1}H NMR (250 MHz, $CDCl_3$) δ (ppm): 7.37 (CH($C_6H_4CH_2S$)); 7.15 (CH(C_6H_4O)); 6.91 (CH(C_6H_4O)); 4.64 (CH_2(C_5H_4CO)); 4.31 (CH-(C_5H_4CO)); 4.19 (Cp); 3.62 (SCH_2−arom.); 2.86 ($SiCH_2N$); 1.27 (CH_2 alkylthiol); 0.89 (CH_3 alkylthiol); 0.08 (CH_3Si). ^{13}C NMR (62.9 MHz, $CDCl_3$) δ(ppm): 170.00 (*C*ONH); 156.41(C(C_6H_4O)); 139.13 (C(SCH_2-(C_6H_4)CH_2)); 129.71 (CH($C_6H_4CH_2S$)); 127.3 (CH(C_6H_4O)); 114.4 (CH(C_6H_4C)); 70.0 (CH(C_5H_4CO)); 69.6 (CH(Cp)); 67.9 (CH(C_5H_4-CO)); 42.0 ($SiCH_2N$); 32.0−29.4 (CH_2 alkylthiol); 28.7 (SCH−arom.); 22.6 (CH_2 alkylthiol); 17.7 (CH_2C−arom.); 15.2 (CH_2CH_2Si); 14.1 (CH_3 alkylthiol); −4.0 (CH_3Si). IR (KBr, cm^{-1}): ν_{CON} 1625.3, 1542.5. $E_{1/2}$ (V vs Fc; CH_2Cl_2; 20 °C) 0.145 (r) (see text and Scheme 4).

Direct Brust Colloid Synthesis. General Method. (a). A colorless solution of N(*n*-C_8H_{17})$_4$Br (0.524 g, 0.959 mmol) in 10 mL of toluene was added to a yellow water solution (10 mL) of $HAuCl_4$ (0.093 g, 0.274 mmol). The mixture was stirred under positive nitrogen pressure, and separation between the red organic phase (top) and colorless aqueous phase (bottom) resulted. A mixture of dodecanethiol $C_{12}H_{25}$-SH (0.028 g, 0.137 mmol) and dendronized-thiol containing the tri-silyl ferrocenyl unit (0.150 g, 0.137 mmol) in 10 mL of toluene was added to the organic phase. Then, $NaBH_4$ (0.114 g, 3.04 mmol) in 10 mL of water was slowly added to the stirred reaction mixture. The red color turned to black brown, and the reaction mixture was vigorously stirred for 3 h. The organic phase was separated from the aqueous phase, its volume was reduced to 3 mL, and 100 mL of ethanol was added. The mixture was kept at −20 °C for 12 h. The resulting dark brown-black precipitate was filtered on Celite and then washed twice with ethanol and twice with acetone to remove excess thiol. The crude product was dissolved in CH_2Cl_2 and precipitated again with methanol.

The dark black colloid containing the mixture of ligands $C_{12}H_{25}S$/dendron-thiol tri-silyl ferrocene = 75:25 (ratio determined by ^{1}H NMR) was then dried under vacuum, which gave 0.085 g. ^{1}H NMR (250 MHz, $CDCl_3$) δ_{ppm}: 7.33 (C*H*($C_6H_4CH_2S$)); 7.21 (C*H*(C_6H_4O)); 6.91 (C*H*(C_6H_4O)); 4.94 (CH_2O); 4.31 (C*H*(C_5H_4Si)); 4.10 (Cp); 4.03 (C*H*(C_5H_4Si)); 3.51 (SCH_2−arom.); 1.27 (CH_2 alkylthiol); 0.89 (CH_3 alkylthiol); 0.62 (CH_2Si); 0.08 (CH_3Si). ^{13}C NMR (62.9 MHz, $CDCl_3$) δ_{ppm}: 156.41 (C(C_6H_4O)); 142.13 (C($SCH_2(C_6H_4)CH_2$)); 133.01 (C*H*($C_6H_4CH_2S$)); 132.3 (C*H*(C_6H_4O)); 112.4 (C*H*(C_6H_4O)); 72.5(CH-(C_5H_4Si)); 70.5 (CH(C_5H_4Si)); 69.6 (CH (Cp)); 63.8 (CH_2O); 31.90−29.4 (CH_2 alkylthiol); 28.82 (SCH−arom.); 22.56 (CH_2 alkylthiol); 17.92 (CH_2C−arom.); 15.23 (CH_2CH_2Si); 14.1 (CH_3 alkylthiol); 3.11 (CH_2CH_2Si); −4.0 (CH_3Si).

(b). A reaction between $HAuCl_4$ (0.031 g, 0.092 mmol), N(*n*-C_8H_{17})$_4$-Br (0.176 g, 0.322 mmol), $C_{12}H_{25}SH$ (0.0094 g 0.046 mmol) dendron **21** (0.150 g, 0.046 mmol), and $NaBH_4$ (aq) solution (0.038 g, 1.00 mmol) was carried out as in procedure (**a**) which gave nanoparticle **24**. ^{1}H NMR integration indicated that the ratio of ligands $C_{12}H_{25}S$ and **21** was 80:20. ^{1}H NMR (250 MHz, $CDCl_3$) δ_{ppm}: 7.33 (C*H*(C_6H_4-CH_2S)); 7.21 (C*H*(C_6H_4O)); 7.01 (C*H*($C_6H_4CH_2S$)); 6.91 (C*H*(C_6H_4O)); 5.05 (CH_2O); 4.29 (C*H*(C_5H_4Si)); 4.10 (Cp); 4.01 (CH(C_5H_4Si)); 3.87 (O−C*H*$_2$); 1.90 (C*H*$_2$); 1.27 (CH_2 alkylthiol); 0.89 (CH_3 alkylthiol); 0.62 (CH_2Si); 0.16 (CH_3Si). ^{13}C NMR (62.9 MHz, $CDCl_3$) δ_{ppm}: 155.91 (C_{qAr}); 139.58 (C_{qAr}); 127.15 (CH_{Ar}); 113.40 (CH_{Ar}); 72.68 (CH (C_5H_4-Si)); 70.5 (CH (C_5H_4Si)); 69.6 (CH (Cp)); 65.52 (CH_2O); 42.94 (C_q−CH_2); 41.89 (CH_2); 29.4 (CH_2 alkylthiol); 17.82; 17.28; 15.03 (CH_2); 14.30 (CH_3 alkylthiol); −2.14.0 (CH_3Si).

(c). Procedure (**a**) applied to the mixture of $HAuCl_4$ (0.029 g, 0.086 mmol), N(*n*-C_8H_{17})$_4$Br (0.165 g, 0.301 mmol), $C_{12}H_{25}SH$ (0.009 g 0.043 mmol), dendron **23** (0.150 g, 0.043 mmol), and aq $NaBH_4$ solution (0.036 g, 0.95 mmol) gave nanoparticle **25**. The proportion of ligands $C_{12}H_{25}S$ and **23** in the mixture was 90:10. ^{1}H NMR (250 MHz, $CDCl_3$) δ_{ppm}: 7.33 (C*H*($C_6H_4CH_2S$)); 7.15 (C*H*(C_6H_4O)); 6.55 (C*H*(C_6H_4O)); 5.05 (CH_2O); 4.29 (C*H*(C_5H_4Si)); 4.08 (Cp); 4.01 (C*H*(C_5H_4Si)); 3.52 (OCH_2); 1.58 (CH_2); 1.27 (CH_2 alkylthiol); 1.14 (CH_2); 0.89 (CH_3 alkylthiol); 0.62 (CH_2Si); 0.16 (CH_3Si). ^{13}C NMR (62.9 MHz, $CDCl_3$) δ_{ppm}: 158.96 (*C*(C_6H_4O)); 139.45 (C_q($SCH_2(C_6H_4)CH_2$); 127.19 (CH_{Ar}); 113.39 (*C*H (C_6H_4O)); 72.90 (*C*H(C_5H_4Si)); 70.57 (*C*H (C_5H_4Si)); 68.07 (CH (Cp)); 60.15 (CH_2O); 43.12 (C_q−CH_2); 42.16 (CH_2); 29.93 (CH_2 alkylthiol); 18.04, 17.52 (CH_2); 14.21 (CH_3 alkylthiol); 3.11 (CH_2CH_2-Si); −1.19 (CH_3Si).

Determination of the Number of Ligands in the Dendronized Gold Nanoparticles. Elemental analysis found for **11**: S, 3.41; Au, 54.68. Atomic ratio Au/S = 2.6. HRTEM: average diameter = 2.3 ± 0.4 nm. Number of gold atoms *per* core: 375. n_s = 144. Proportion of dendron **8** = 25%. Average number of dendron **8** *per* particle: $n_{dendron\mathbf{8}}$ = 36; $n_{alkylthiolate}$ = 108. MW = 135 072 g/mol.

Elemental analysis found for **12**: S, 4.39; Au, 67.52. Atomic ratio Au/S = 2.5. HRTEM: average diameter = 2.3 ± 0.7 nm. Number of gold atoms *per* core: 375. n_s = 150. Proportion of dendrons **10** = 3%. Average number of dendron **10** *per* particle: $n_{dendron\mathbf{10}}$ = 4.5; $n_{alkylthiolate}$ = 145.5. MW = 108 868 g/mol.

Elemental analysis found for **25**: S, 2.53; Au, 57.68. This elemental analysis provides the atomic ratio Au/S = 3.7 = *X*. HRTEM: average diameter *D* (gold core): 2.9 ± 0.5 nm. Number of gold atoms *per* core:[34] $N_{Au} = 4\pi R^3/3\nu_g = 4\pi(D/2)^3/51 = 751$ Au atoms *per* particle in average (ν_g = 17 Å^3 for a gold atom). The number n_s of thiolate ligand *per* particle can then be deduced: $n_s = N_{Au}/X = 751/3.7 = 203$. The proportion of dendron **23** is given by the ^{1}H NMR spectrum of **25**: 10%. The average number of dendron **23** *per* particle is $n_{dendron\mathbf{23}}$ = 10/100 × 203 = 20.3 The average number of remaining dodecanethiolate ligands is $n_{alkylthiolate}$ = 203 − 20.3 = 182.7. The average molecular weight *per* dendronized particle is MW = N_{Au} × 196.97 + $n_{dendron}MW_{dendron} + n_{alkylthiolate}MW_{alkylthiolate}$ = 254 157 g/mol.

Elemental analysis found for **24**: S, 2.25; Au, 42.80. Atomic ratio Au/S = 3.1. HRTEM: average diameter: 2.8 ± 0.5 nm. Number of gold atoms *per* core: 676. n_s = 218. Proportion of dendron **21** = 20%. The average number of dendron **21** *per* particle is $n_{dendron21}$ = 43.6; $n_{alkylthiolate}$ =174.4. MW = 309 806 g/mol.

General Method for the Titration of $H_2PO_4^-$ or ATP^{2-}: First, [*n*-Bu_4N][PF_6] was introduced in the electrochemical cell (that contained the working electrode, the reference electrode, and the counter electrode) and dissolved in freshly distilled dichloromethane. A blank voltammogram was recorded without colloid in order to check the working electrode. Then, the colloid was solubilized in a minimum of dichloromethane and added into the cell. About 1 mg (3 × 10^{-6} mol) of decamethylferrocene was also added. After the solution was degassed by dinitrogen flushing, the CV of the nanoparticle alone was recorded. Then, the anion $H_2PO_4^-$ or ATP^{2-} was added by small quantities using a microsyringe. After each addition, the solution was degassed, and a CV was recorded. The appearance and progressive increase of a new wave was observed while the initial wave decreased and finally disappeared (see all the titration graphs in the Supporting Information). When the initial wave had completely disappeared, addition of the salt of the anion was continued until reaching twice the volume already introduced. The titration of ATP^{2-} in the presence of Cl^- and HSO_4^- was carried out similarly, the salts [*n*-Bu_4N][Cl] and [*n*-Bu_4N][HSO_4] being added before [*n*-Bu_4N]$_2$[ATP].

Modification of Electrodes with the Dendronized Gold Nanoparticles. A platinum electrode (Sodimel, Pt 30) was dipped into 10% aq HNO_3 for 3 h, then rinsed with distilled water, dried in air, and polished using cerium oxide pulver (5 MU). The nanoparticles were electrodeposited onto such platinum-disk electrodes (A = 0.078 cm^2) from degassed CH_2Cl_2 solutions of metallodendron gold nanoparticles (10^{-6} M) and [*n*-Bu_4N][PF_6] (0.1 M) by continuous scanning (0.10 V s^{-1}) up to 50 cycles between 0.0 and 0.80 V vs FeCp*$_2$. The coated electrode was washed with CH_2Cl_2 in order to remove the solution of material and dried in air. This modified electrode was characterized by CV in freshly distilled CH_2Cl_2 as containing only the supporting electrolyte. It showed a single symmetrical CV wave, and the linear relationship of the peak current with potential sweep rate was verified. The surface coverage Γ (mol cm^{-2}) by the dendronized gold nanoparticles was determined from the integrated charge of the CV wave. $\Gamma = Q/nFA$, where Q is the charge, n is the number of electrons transferred, F is the Faraday constant, and A is the area. Thus, the surface coverage for the electrode modified with **12** was 2.3 × 10^{-10} mol cm^{-2} (ferrocenyl sites), corresponding to 1.7 × 10^{-11} mol cm^{-2} of colloid-3-amido-Fc. The coverage surface Γ for the electrode modified with **24** was 5.6 × 10^{-10} mol cm^{-2} (ferrocenyl sites) or 1.55 × 10^{-12} mol cm^{-2} of colloid-9-silyl-Fc **24**. The nanoparticle **25** electrodeposited onto the Pt-disk electrode showed a surface coverage of Γ = 1× 10^{-10} mol cm^{-2}, corresponding to a number of colloid-9-silyl-silyl-Fc **25** of 5.5 × 10^{-13} mol cm^{-2}.

Acknowledgment. We are grateful to Prof. J.-C. Moutet (University of Grenoble) for helpful discussions and the Institut Universitaire de France (IUF, grant to D. A.), the Centre National de la Recherche Scientifique (CNRS), the Ministère de la Recherche et de la Technologie (MRT, Ph. D. grant to M.-C. D.), and the Universities Bordeaux I and Paris VI for financial support.

Supporting Information Available: Syntheses of the AB_3 derivatives leading to thiols containing three ferrocenyl groups; histograms and TEM pictures of the dendronized gold nanoparticles (Figures SI 1 to SI 4) and CVs (Figures SI 5 and SI 6) and graphs of current variations (Figures SI 7 to SI 13) for the anion titrations by the dendronized gold nanoparticles. This material is available free of charge via the Internet at http://pubs.acs.org.

JA021325D

(34) Leff, D. V.; Ohara, P. C.; Heath, J. R.; Gelbart, W. M. *J. Phys. Chem.* **1995**, 99, 7036.